



Efficient stability and vibration analysis of an all-steel modular floor assembly

Rajshri Chidambaram Muthu Kumar¹, Bayley P. St. Jacques², Sándor Ádány³,
Onur Avci⁴, Jerome F. Hajjar⁵, Benjamin W. Schafer⁶

Abstract

The objective of this paper is to document and validate the extension of an open source finite strip method stability software (CUFSM) to include vibration analysis, and to demonstrate the application of the resulting solution to assess the stability and vibration of a prototype all-steel modular floor assembly. Currently, the open source finite strip software CUFSM performs stability analysis of thin-walled members, providing eigen buckling loads and the corresponding buckling mode shapes. The same framework and solvers may readily be extended to vibration analysis, as both are eigenvalue problems, and thus the extended software can provide eigen frequencies and the corresponding vibration mode shapes. The vibration implementation is verified against existing vibration frequency solutions for plates and beams. To demonstrate the efficiency of having both stability and vibration solutions readily at hand, preliminary assessment of a floor assembly is performed for a variety of parameters, e.g., beam size, plate thickness, and attachment assumptions using the finite strip method as implemented in a custom version of CUFSM. The work is part of a larger effort that is also investigating detailed shell finite element models, experimental strength, vibration, and acoustical assessments of the floor assembly.

1. Introduction

Assessment of steel structures requires fully understanding their strength and serviceability performance. For slender structures, stability is a critical consideration and numerically efficient tools to assess cross-section and member stability utilizing the finite strip method, such as CUFSM (Schafer et al., 2006), or THIN-WALL (Hancock et al., 2022), have been effectively utilized by practicing engineers and are even referenced in national design specifications (e.g., AISI S100, Aluminum Design Manual, AISC 370). As we optimize for material efficiency, serviceability limit states often take priority, and additional assessment, for example in vibration is required. Utilizing

¹ Graduate Research Assistant, Johns Hopkins University, <rchidam3@jhu.edu>

² Graduate Research Assistant, Northeastern University, <st.jacques.b@northeastern.edu>

³ Professor, Budapest University of Technology and Economics, <adany.sandor@emk.bme.hu>
Visiting Faculty Scholar, Johns Hopkins University, <asandor2@jhu.edu>

⁴ Assistant Professor, West Virginia University, <onur.avci@mail.wvu.edu>

⁵ Professor, Northeastern University, <jf.hajjar@northeastern.edu>

⁶ Professor, Johns Hopkins University, <schafer@jhu.edu>

the same model for stability and vibration assessment has inherent advantages for efficiency and could more readily allow for coupled stability-vibration optimization.

This paper first provides a background to the stability assessment of members using the finite strip method as implemented in the software CUFSM. This is followed by the extension of the solution to vibration, based on the classical derivations in Cheung et al., 1998. To validate the developed solution the numerically predicted vibration frequencies are compared with solutions in the literature for plates and beams. Finally, a prototype all-steel floor assembly appropriate for commercial structural steel construction is introduced. The assembly is then assessed for both stability and vibration utilizing the developed extensions to CUFSM.

2. Finite strip stability background

CUFSM, an open-source software published by the senior author that's available online has both GUI and MATLAB versions (Schafer et al., 2006). This software performs the buckling analysis of steel cross-sections and for beams; it can provide the critical buckling moments for local, distortional, and global buckling. The finite strip method uses strips along the longitudinal direction of the cross-section. Trigonometric shape functions (Y_m 's) are employed for the longitudinal direction, and they vary based on the type of the prescribed end boundary condition: simple-simple, clamped-clamped, simple-clamped, clamped-free or clamped-guided. For the transverse direction of the strip, classical cubic polynomial shape functions are used. The coordinates, degrees of freedom and loads on a typical strip are shown below.

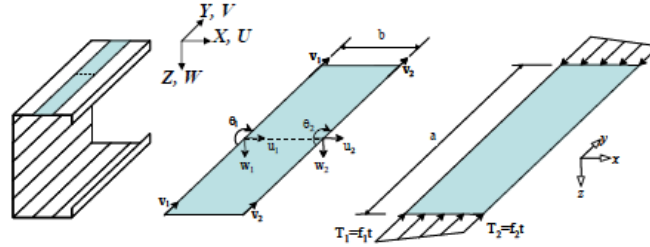


Figure 1: Coordinates, Degrees of Freedom, and loads of a typical strip (Li et al., 2010)

Within a strip, local displacement fields u , v , and w are expressed by the linear combination of basis functions and the nodal displacements, which latter ones now should be interpreted as characteristic displacement values at nodal lines. In the classic FSM the displacements are interpolated as follows:

$$u(x, y) = \sum_{m=1}^q \left[\left(1 - \frac{x}{b}\right) \quad \left(\frac{x}{b}\right) \right] \begin{bmatrix} u_{1[m]} \\ u_{2[m]} \end{bmatrix} Y_{[m]} \quad (2.1)$$

$$v(x, y) = \sum_{m=1}^q \left[\left(1 - \frac{x}{b}\right) \quad \left(\frac{x}{b}\right) \right] \begin{bmatrix} v_{1[m]} \\ v_{2[m]} \end{bmatrix} \frac{Y'_{[m]}}{c_{[m]}} \quad (2.2)$$

$$w(x, y) = \sum_{m=1}^q \left[\left(1 - \frac{3x^2}{b^2} + \frac{2x^3}{b^3}\right) \quad \left(x - \frac{2x^2}{b} + \frac{x^3}{b^2}\right) \quad \left(\frac{3x^2}{b^2} - \frac{2x^3}{b^3}\right) \quad \left(\frac{x^3}{b^2} - \frac{x^2}{b}\right) \right] \begin{bmatrix} w_{1[m]} \\ \theta_{1[m]} \\ w_{2[m]} \\ \theta_{2[m]} \end{bmatrix} Y_{[m]} \quad (2.3)$$

where $c_{[m]} = m\pi/a$, and a is the member length, b is the strip width, and q is the number of considered terms.

The longitudinal shape functions, $Y_{[m]}$, for the different boundary conditions utilized in both the elastic stiffness matrix and the consistent mass matrix are as follows:

$$\text{Simple-simple (S-S)} : Y_{[m]} = \sin\left(\frac{m\pi y}{a}\right) \quad (2.4)$$

$$\text{Clamped-clamped (C-C)} : Y_{[m]} = \sin\left(\frac{m\pi y}{a}\right) \sin\left(\frac{\pi y}{a}\right) \quad (2.5)$$

$$\text{Simple-clamped (S-C)} : Y_{[m]} = \sin\left[\frac{(m+1)\pi y}{a}\right] + \left(m + \frac{1}{m}\right) \sin\left(\frac{m\pi y}{a}\right) \quad (2.6)$$

$$\text{Clamped-free (C-F)} : Y_{[m]} = 1 - \cos\left[\frac{\left(m-\frac{1}{2}\right)\pi y}{a}\right] \quad (2.7)$$

$$\text{Clamped-guided (C-G)} : Y_{[m]} = \sin\left[\frac{\left(m-\frac{1}{2}\right)\pi y}{a}\right] \sin\left(\frac{\pi y}{a}\right) \quad (2.8)$$

There are four degrees of freedom per longitudinal term which comprises of two in-plane (membrane) degrees of freedom (u, v) and two out-of-plane (bending) degrees of freedom (w, θ) as shown in Fig. 1. (Note that Fig. 1 illustrates the nodal displacements for the simplest longitudinal shape function, i.e., $Y_{[m]} = \sin\frac{m\pi y}{a}$, with $[m]=1$.) Accordingly, the d displacement vector for a strip is as follows:

$$d^T = [d_{[1]}^T \quad \cdots \quad d_{[m]}^T \quad \cdots \quad d_{[n]}^T \quad \cdots \quad d_{[q]}^T] \quad (2.9)$$

where $[m]$ and $[n]$ are referring to the m^{th} and n^{th} term in the longitudinal function series, and within an 8-element sub-vector the order of nodal displacement is assumed as follows:

$$d_{[m]} = [u_{1[m]} \quad v_{1[m]} \quad u_{2[m]} \quad v_{2[m]} \quad w_{1[m]} \quad \theta_{1[m]} \quad w_{2[m]} \quad \theta_{2[m]}]^T \quad (2.10)$$

Thus, the membrane DOFs are the first 4 entries and the bending DOFs are the last 4 entries. The stiffness matrices can be derived by following the usual steps, as detailed in Li et al., 2011. The stiffness matrix of a strip consists of $q \times q$ sub-matrices, as follows:

$$k = \begin{bmatrix} k_{[11]} & \cdots & k_{[1m]} & \cdots & k_{[1n]} & \cdots & k_{[1q]} \\ \vdots & \ddots & & & & & \vdots \\ k_{[m1]} & & k_{[mm]} & & k_{[mn]} & & k_{[mq]} \\ \vdots & & & \ddots & & & \vdots \\ k_{[n1]} & & k_{[nm]} & & k_{[nn]} & & k_{[nq]} \\ \vdots & & & & & \ddots & \vdots \\ k_{[q1]} & \cdots & k_{[qm]} & \cdots & k_{[qn]} & \cdots & k_{[qq]} \end{bmatrix} \quad (2.11)$$

where $[m]$ and $[n]$ are as defined in the displacement vector $d_{[m]}$, and q is the number of considered terms. The sub-matrices are 8×8 . According to the assumed DOF order, each sub-matrix of the stiffness matrix can be composed of 4 partitions as follows:

$$k_{[mn]} = \begin{bmatrix} k_{em[mn]} & 0 \\ 0 & k_{eb[mn]} \end{bmatrix} \quad (2.12)$$

where the ‘ em ’ partition (4×4) belongs to the membrane behavior, the ‘ eb ’ partition (4×4) belongs to the bending behavior, while the out-of-diagonal partitions (which account for the coupling between membrane and bending behaviors) are zero.

The membrane and bending partitions of $k_{[mn]}$ are expressed as follows

$$k_{em[mn]} = t \int_0^a \int_0^b N_{uv[m]}^T L_{uv}^T E_m L_{uv} N_{uv[n]} dx dy \quad (2.13)$$

$$k_{eb[mn]} = \int_0^a \int_0^b N_{w\theta[m]}^T L_{w\theta}^T E_b L_{w\theta} N_{w\theta[n]} dx dy \quad (2.14)$$

with the L operator matrices:

$$L_{uv} = \begin{bmatrix} \frac{\partial}{\partial x} & 0 \\ 0 & \frac{\partial}{\partial y} \\ \frac{\partial}{\partial y} & \frac{\partial}{\partial x} \end{bmatrix} \quad L_{w\theta} = \begin{bmatrix} -\frac{\partial^2}{\partial x^2} \\ -\frac{\partial^2}{\partial y^2} \\ -2\frac{\partial^2}{\partial x \partial y} \end{bmatrix} \quad (2.15)$$

and N matrices for the interpolation functions:

$$[N_{uv[m]}] = \begin{bmatrix} \left(1 - \frac{x}{b}\right) Y_{[m]} & 0 & \frac{x}{b} Y_{[m]} & 0 \\ 0 & \left(1 - \frac{x}{b}\right) \frac{Y_{[m]}'}{c_{[m]}} & 0 & \frac{x}{b} \frac{Y_{[m]}'}{c_{[m]}} \end{bmatrix} \quad (2.16)$$

$$[N_{w\theta[m]}] = \left[\left(1 - \frac{3x^2}{b^2} + \frac{2x^3}{b^3}\right) \quad \left(x - \frac{2x^2}{b} + \frac{x^3}{b^2}\right) \quad \left(\frac{3x^2}{b^2} - \frac{2x^3}{b^3}\right) \quad \left(\frac{x^3}{b^2} - \frac{x^2}{b}\right) \right] Y_{[m]} \quad (2.17)$$

where $c_{[m]} = \frac{m\pi}{a}$, $c_{[n]} = \frac{n\pi}{a}$ and $[N_{uv[n]}]$ and $[N_{w\theta[n]}]$ are expressed the same way by replacing $[m]$ with $[n]$.

For the assumed orthotropic material, the material matrices are expressed as:

$$E_m = \begin{bmatrix} \frac{E_x}{1 - \nu_x \nu_y} & \frac{E_x \nu_y}{1 - \nu_x \nu_y} & 0 \\ \frac{E_y \nu_x}{1 - \nu_x \nu_y} & \frac{E_y}{1 - \nu_x \nu_y} & 0 \\ 0 & 0 & G \end{bmatrix} = \begin{bmatrix} E_1 & E_1 \nu_y & 0 \\ E_2 \nu_x & E_2 & 0 \\ 0 & 0 & G \end{bmatrix} \quad (2.18)$$

$$E_b = \frac{t^3}{12} E_m = \begin{bmatrix} D_x & D_1 & 0 \\ D_2 & D_y & 0 \\ 0 & 0 & D_{xy} \end{bmatrix} \quad (2.19)$$

where E_x and E_y are the modulus of elasticity in the x and y direction, respectively, ν_x and ν_y are the Poisson's ratio in the x and y direction, respectively, while G is the shear modulus. Moreover, in realistic materials $E_1 \nu_y = E_2 \nu_x$, hence $D_1 = D_2$.

After performing differentiations and integrations the strip stiffness matrices can be expressed analytically, as follows:

$$k_{em} = t \begin{bmatrix} \left(\frac{E_1 I_1}{b} + \frac{G b I_5}{3} \right) & \left(-\frac{E_2 \nu_x I_3}{2c_{[m]}} - \frac{G I_5}{2c_{[n]}} \right) & \left(-\frac{E_1 I_1}{b} + \frac{G b I_5}{6} \right) & \left(-\frac{E_2 \nu_x I_3}{2c_{[n]}} + \frac{G I_5}{2c_{[n]}} \right) \\ \left(-\frac{E_2 \nu_x I_2}{2c_{[m]}} - \frac{G I_5}{2c_{[m]}} \right) & \left(\frac{E_2 b I_4}{3c_{[m]} c_{[n]}} + \frac{G I_5}{b c_{[m]} c_{[n]}} \right) & \left(\frac{E_2 \nu_x I_2}{2c_{[m]}} - \frac{G I_5}{2c_{[m]}} \right) & \left(\frac{E_2 b I_4}{6c_{[m]} c_{[n]}} - \frac{G I_5}{b c_{[m]} c_{[n]}} \right) \\ \left(-\frac{E_1 I_1}{b} + \frac{G b I_5}{6} \right) & \left(\frac{E_2 \nu_x I_3}{2c_{[n]}} - \frac{G I_5}{2c_{[n]}} \right) & \left(\frac{E_1 I_1}{b} + \frac{G b I_5}{3} \right) & \left(\frac{E_2 \nu_x I_3}{2c_{[n]}} + \frac{G I_5}{2c_{[n]}} \right) \\ \left(-\frac{E_2 \nu_x I_2}{2c_{[m]}} + \frac{G I_5}{2c_{[m]}} \right) & \left(\frac{E_2 b I_4}{6c_{[m]} c_{[n]}} - \frac{G I_5}{b c_{[m]} c_{[n]}} \right) & \left(\frac{E_2 \nu_x I_2}{2c_{[m]}} + \frac{G I_5}{2c_{[m]}} \right) & \left(\frac{E_2 b I_4}{3c_{[m]} c_{[n]}} + \frac{G I_5}{b c_{[m]} c_{[n]}} \right) \end{bmatrix}$$

$$k_{eb} = \frac{1}{420b^3} \begin{bmatrix} \begin{pmatrix} 5040D_x I_1 - 504b^2 D_1 I_2 \\ -504b^2 D_1 I_3 + 156b^4 D_y I_4 \\ +2016b^2 D_{xy} I_5 \end{pmatrix} & \begin{pmatrix} 2520b D_x I_1 - 462b^3 D_1 I_2 \\ -42b^3 D_1 I_3 + 22b^5 D_y I_4 \\ +168b^3 D_{xy} I_5 \end{pmatrix} & \begin{pmatrix} -5040D_x I_1 + 504b^2 D_1 I_2 \\ +504b^2 D_1 I_3 + 54b^4 D_y I_4 \\ -2016b^2 D_{xy} I_5 \end{pmatrix} & \begin{pmatrix} 2520b D_x I_1 - 42b^3 D_1 I_2 \\ -42b^3 D_1 I_3 - 13b^5 D_y I_4 \\ +168b^3 D_{xy} I_5 \end{pmatrix} \\ \begin{pmatrix} 2520b D_x I_1 - 462b^3 D_1 I_2 \\ -42b^3 D_1 I_2 + 22b^5 D_y I_4 \\ +168b^3 D_{xy} I_5 \end{pmatrix} & \begin{pmatrix} 1680b^2 D_x I_1 - 56b^4 D_1 I_2 \\ -56b^4 D_1 I_3 + 4b^6 D_y I_4 \\ +224b^4 D_{xy} I_5 \end{pmatrix} & \begin{pmatrix} -2520b D_x I_1 + 42b^3 D_1 I_2 \\ +42b^3 D_1 I_2 + 13b^5 D_y I_4 \\ -168b^3 D_{xy} I_5 \end{pmatrix} & \begin{pmatrix} 840b^2 D_x I_1 + 14b^4 D_1 I_2 \\ +14b^4 D_1 I_3 - 3b^6 D_y I_4 \\ -56b^4 D_{xy} I_5 \end{pmatrix} \\ \begin{pmatrix} -5040D_x I_1 + 504b^2 D_1 I_2 \\ +504b^2 D_1 I_3 + 54b^4 D_y I_4 \\ -2016b^2 D_{xy} I_5 \end{pmatrix} & \begin{pmatrix} -2520b D_x I_1 + 42b^3 D_1 I_2 \\ +42b^3 D_1 I_3 + 13b^5 D_y I_4 \\ -168b^3 D_{xy} I_5 \end{pmatrix} & \begin{pmatrix} 5040D_x I_1 - 504b^2 D_1 I_2 \\ -504b^2 D_1 I_3 + 156b^4 D_y I_4 \\ +2016b^2 D_{xy} I_5 \end{pmatrix} & \begin{pmatrix} -2520b D_x I_1 + 462b^3 D_1 I_2 \\ +42b^3 D_1 I_3 - 22b^5 D_y I_4 \\ -168b^3 D_{xy} I_5 \end{pmatrix} \\ \begin{pmatrix} 2520b D_x I_1 - 42b^3 D_1 I_2 \\ -42b^3 D_1 I_3 - 13b^5 D_y I_4 \\ +168b^3 D_{xy} I_5 \end{pmatrix} & \begin{pmatrix} 840b^2 D_x I_1 + 14b^4 D_1 I_2 \\ +14b^4 D_1 I_3 - 3b^6 D_y I_4 \\ -56b^4 D_{xy} I_5 \end{pmatrix} & \begin{pmatrix} -2520b D_x I_1 + 462b^3 D_1 I_2 \\ +42b^3 D_1 I_2 - 22b^5 D_y I_4 \\ -168b^3 D_{xy} I_5 \end{pmatrix} & \begin{pmatrix} 1680b^2 D_x I_1 - 56b^4 D_1 I_2 \\ -56b^4 D_1 I_3 + 4b^6 D_y I_4 \\ +224b^4 D_{xy} I_5 \end{pmatrix} \end{bmatrix}$$

where the integrals I_1 through I_5 are as follows: $I_1 = \int_0^a Y_m Y_n dy$, $I_2 = \int_0^a Y_m'' Y_n dy$, $I_3 = \int_0^a Y_m Y_n'' dy$, $I_4 = \int_0^a Y_m'' Y_n'' dy$, and $I_5 = \int_0^a Y_m' Y_n' dy$. Closed-form solutions are provided in Li et al., 2011.

The strip geometric stiffness matrix, k_g , is formed from consideration of the higher order strain terms and the resulting external work created under the applied end tractions T_1 and T_2 as shown in Fig. 1. Since the k_g matrix is not used in the vibration solution, which is the focus of the work reported here, see Li et al., 2011 for the solution.

The global elastic and geometric stiffness matrices are obtained from the local stiffness matrices through transformation of the strip from local to global coordinates and assembly into the global matrix based on the global DOF numbering scheme. For CUFSM the stability solution is of critical importance and this assembly is used to solve the following eigenvalue problem:

$$([\mathbf{K}] - \lambda[\mathbf{K}_g])\{\phi\} = \{0\} \quad (2.20)$$

where $[\mathbf{K}]$ is the elastic stiffness matrix, $[\mathbf{K}_g]$ is the geometric stiffness matrix (linearly dependent on the applied stress), λ is the load factor that provides the ratio of the critical buckling stress to the applied stress, and ϕ is the buckled shape associated with the eigenvalue λ .

3. Finite strip vibration derivation

Rather than solve the eigenvalue problem associated with static equilibrium, we form the expression for the equations of motion and solve the free vibration problem, which results in a companion problem to Eq. 2.20, the vibration eigenvalue problem:

$$([\mathbf{K}] - \omega^2[\mathbf{M}])\{\psi\} = \{0\} \quad (3.1)$$

where $[\mathbf{K}]$ is the elastic stiffness matrix formed identically to the stability problem, $[\mathbf{M}]$ is the mass matrix, ω is the natural circular frequency (rad/sec), and ψ is the corresponding mode shape associated with the vibration frequency. Given the established coordinate systems, degrees of freedom, and displacement functions the only term to be derived is $[\mathbf{M}]$.

Two different forms of $[\mathbf{M}]$ are commonly employed: lumped and consistent. The lumped mass matrix assumes only diagonal terms at the DOF. This simplification is particularly advantageous when the resulting mass matrix has to be inverted. However, this is not the case for the eigen vibration problem, therefore the more complete consistent mass matrix is the focus here. The derivation herein closely follows that originally developed by Cheung et al., 1998 and extended here to the specific notation and longitudinal shape functions implemented in CUFSM.

For a strip, like the stiffness matrix, the strip mass matrix consists of $q \times q$ blocks,

$$M = \begin{bmatrix} M_{[11]} & \cdots & M_{[1m]} & \cdots & M_{[1n]} & \cdots & M_{[1q]} \\ \vdots & \ddots & & & & & \vdots \\ M_{[m1]} & & M_{[mm]} & & M_{[mn]} & & M_{[mq]} \\ \vdots & & & \ddots & & & \vdots \\ M_{[n1]} & & M_{[nm]} & & M_{[nn]} & & M_{[nq]} \\ \vdots & & & & & \ddots & \vdots \\ M_{[q1]} & \cdots & M_{[qm]} & \cdots & M_{[qn]} & \cdots & M_{[qq]} \end{bmatrix} \quad (3.2)$$

Each block is partitioned, the out-of-diagonal partitions being zero, while the diagonal partitions corresponding to the in-plane (membrane) mass matrix $[M_{em}]$ associated with local u, v DOF, and the out-of-plane (bending) mass matrix $[M_{eb}]$ associated with the local w, θ DOF:

$$M_{[mn]} = \begin{bmatrix} M_{em[mn]} & 0 \\ 0 & M_{eb[mn]} \end{bmatrix} \quad (3.3)$$

The diagonal partitions can be calculated from the integral expressions as follows:

$$[M_{em[mn]}] = \int_0^a \int_0^b \rho t [N_{uv[m]}]^T [N_{uv[n]}] dx dy \quad (3.4)$$

$$[M_{eb[mn]}] = \int_0^a \int_0^b \rho t [N_{w\theta[m]}]^T [N_{w\theta[n]}] dx dy \quad (3.5)$$

where ρ is the strip density, t is the strip thickness. Note, ρt is assumed to be constant within a strip.

Note, some care must be taken to interpret the expressions due to the typical use of m as the number of terms in the longitudinal shape function expansion and the common use of “ m ” to designate mass. Here uppercase $[M]$ is always used for mass, even when the mass matrix is only for the strip and lower case $[m]$ designates the specific longitudinal terms in an expansion and subscript “ em ” denotes the membrane mass terms in exact parallel to the elastic membrane stiffness matrices.

Solution results in the following form:

$$[M_{em[mn]}] = \rho t \begin{bmatrix} \frac{bI_1}{3} & 0 & \frac{bI_1}{6} & 0 \\ 0 & \frac{bI_5}{3c_{[m]}c_{[n]}} & 0 & \frac{bI_5}{6c_{[m]}c_{[n]}} \\ \frac{bI_1}{6} & 0 & \frac{bI_1}{3} & 0 \\ 0 & \frac{bI_5}{6c_{[m]}c_{[n]}} & 0 & \frac{bI_5}{3c_{[m]}c_{[n]}} \end{bmatrix}$$

$$[M_{eb}] = \rho t \begin{bmatrix} \frac{13bI_1}{35} & \frac{11b^2I_1}{210} & \frac{9bI_1}{70} & -\frac{13b^2I_1}{420} \\ \frac{11b^2I_1}{210} & \frac{b^3I_1}{105} & \frac{13b^2I_1}{420} & -\frac{3b^3I_1}{420} \\ \frac{9bI_1}{70} & \frac{13b^2I_1}{420} & \frac{13bI_1}{35} & -\frac{11b^2I_1}{210} \\ -\frac{13b^2I_1}{420} & -\frac{3b^3I_1}{420} & -\frac{11b^2I_1}{210} & \frac{b^3I_1}{105} \end{bmatrix}$$

The, I , integral solutions in the consistent strip mass matrix are a function of the selected longitudinal shape function.

The mass matrix only requires solution to two of the five integrals utilized in the stiffness matrix, so fully explicit forms for $[M]$ can be found utilizing the following (Li et al., 2011):

	$I_1 = \int_0^a Y_m Y_n dy$	$I_5 = \int_0^a Y_m' Y_n' dy$
S-S	0 except $\frac{a}{2}$ ($m = n$)	0 except $\frac{\pi^2 m^2}{2a}$ ($m = n$)
C-C	$\frac{a}{4}(m = n)$ except $\frac{3a}{8}(m = n = 1)$; $-\frac{a}{8}(m - n = 2)$	$\frac{\pi^2(m+1)^2}{4a}$ ($m = n$); $-\frac{\pi^2(mn+1)}{8a}$ ($ m - n = 2$)
S-C	$\frac{\left[1 + \frac{(m+1)^2}{m^2}\right]a}{2}$ ($m = n$); $\frac{(m+1)a}{2m}$ ($m - n = 1$); $\frac{(n+1)a}{2n}$ ($m - n = -1$)	$\frac{\pi^2(m+1)^2}{a}$ ($m = n$); $\frac{\pi^2(m+1)(n+1)}{2a}$ ($ m - n = 1$)
C-F	$\frac{3a}{2} - \frac{2a(-1)^{m-1}}{\pi(m-\frac{1}{2})}$ ($m = n$); $a - a(-1)^{m-1}/\pi/(m-1/2) - a(-1)^{n-1}/\pi/(n-1/2)$ ($m \neq n$)	$\frac{\pi^2(m-\frac{1}{2})^2}{2a}$ ($m = n$)
C-G	$\frac{a}{4}(m = n)$ except $\frac{3a}{8}(m = n = 1)$; $-\frac{a}{8}(m - n = 2)$	$\frac{\pi^2(m-\frac{1}{2})^2}{4a} + \frac{\pi^2}{16a}$ ($m = n$); $-\frac{\pi^2 n^2}{8a}$ ($m - n = 1$); $-\frac{\pi^2 m^2}{8a}$ ($m = n = -1$)

Assembly of the global mass matrix $[M]$ from the local strips $[M]$ follows the same local to global transformation and assembly based on DOF ordering as for the strip stiffness matrices.

Similar to the signature curve analysis in stability, vibration analysis is also “special” for the simple-simple end boundary condition. The orthogonality property for this case leads to all the integrals becoming zero except the main diagonal in the mass matrix $[M]$ and the elastic stiffness matrix $[K]$. The orthogonality property poses the advantage of using a single longitudinal term $[m]$ to obtain accurate results in a simply supported end boundary condition. However, the orthogonality properties are not applicable to any other boundary conditions. This results in the requirement to use multiple longitudinal terms for all the other boundary conditions to achieve accurate vibration frequencies, similar to stability analysis.

From an implementation standpoint the global elastic element stiffness matrix $[K]$ is already present in CUFSM, so only the addition of $[M]$ is required. The mass matrix $[M]$ and the elastic stiffness matrix $[k_e]$ is generated for each strip in the local coordinates and the resulting element stiffness and mass matrices are transferred to the global coordinate system using the existing subroutines in CUFSM. The strip stiffness and mass matrices are transformed and assembled from the strips into the global stiffness matrix $[K]$ and the global mass matrix $[M]$ using existing routines. Finally, in the eigenvalue solver $[K_g]$ is replaced by $[M]$. Care must be taken with the

squared term in the eigenvalue output, otherwise the results are without change. The only new information required to perform the analysis is the density of each strip, ρ .

4. Validation

This section provides the validation for the above derived finite strip method for vibration frequencies. The results from CUFSM are compared with theoretical vibration frequencies for a rectangular plate that is simply supported on all edges, a square plate fixed on all edges, a simply supported beam, and a cantilevered beam.

4.1 Rectangular plate simply supported on all edges

A rectangular plate with a width, b , of 100 in., a uniform thickness, t , of 0.1 in., a density, ρ , of 7.5×10^{-7} kip-s²/in.⁴ and varying length, a , is studied. The plate is modeled with isotropic material $E = 29000$ ksi, $\nu=0.3$. in CUFSM the end boundary condition is specified as ‘S-S’ and the nodes at the ends of the cross-section are defined with fixed degrees of freedom in the horizontal (x DOF) and vertical direction (z DOF) to account for the plate being simply supported on all the edges. The plate is modeled with ten strips.

On performing the finite strip vibration analysis, the results for the mode shapes corresponding to $m=1$ and $n=1,2$, where here m and n refer to the number of observed half-waves in the longitudinal and transverse directions, as shown in Fig. 2 and Fig. 3 and the vibration frequencies obtained are 1.87 Hz (11.8 rad/sec) and 4.71 Hz (29.6 rad/sec) respectively.

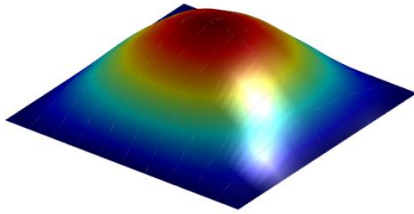


Figure 2: Mode shape for $a/b=1$, $(m,n)=1,1$

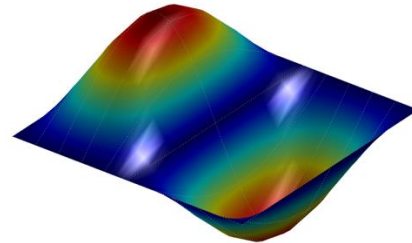


Figure 3: Mode shape for $a/b=1$, $(m,n)=1,2$

The analytical solution for vibration frequency ω_{mn} of a plate simply supported on all edges (from Szilard et al., 2004) is:

$$\omega_{mn}(\text{rad/sec}) = \sqrt{\frac{D}{\rho t} \left(\frac{m^2 \pi^2}{a^2} + \frac{n^2 \pi^2}{b^2} \right)} \quad (4.1)$$

where D is the plate rigidity $Et^3/(12(1-\nu^2))$. Vibration frequencies for different modes and different lengths of the plate are obtained and compared with the analytical solution as shown in Table 4. The results from CUFSM are found to be in close agreement with the theoretical solutions, even with only ten strips.

Table 4: Comparison between CUFSM and theoretical vibration frequencies for a SS plate

a/b	(m, n)	Vibration Frequencies (rad/s)	
		CUFSM	Theoretical
0.5	(1,1)	29.8	29.6
	(1,2)	47.6	47.3
	(1,3)	77.5	76.9
	(2,1)	101.5	100.6
1	(1,1)	11.8	11.8
	(1,2)	29.6	29.6
	(1,3)	59.6	59.2
	(2,1)	29.6	29.6
2	(1,1)	7.3	7.4
	(1,2)	25.2	25.1
	(1,3)	55.1	54.7
	(2,1)	11.7	11.8

For varying length, or aspect ratio, the non-dimensional vibration frequency f_{mn} (defined below) corresponding to CUFSM (from the vibration frequencies obtained through finite strip analysis) and the analytical solution are plotted with respect to a/b in Fig. 4. This is analogous to the Garland curves (Timoshenko et al., 1962) in the case of plate buckling. The two non-dimensional frequencies are:

$$CUFSM: f_{mn} = \frac{\omega_{mn}}{\frac{\pi^2}{b^2} \sqrt{\frac{D}{\rho t}}} \quad (4.2)$$

$$Analytical: f_{mn} = \left(m^2 \left(\frac{b}{a} \right)^2 + n^2 \right) \quad (4.3)$$

Fig. 4 provides the CUFSM solution for f_{mn} for a single half-wavelength (longitudinal term, $m=1$) with the theoretical solution. The results for the first four mode shapes ($n=1$ to 4) corresponding to a single longitudinal half-wavelength ($m=1$) for varying aspect ratios ($a/b=1$ to 10) for a simply supported rectangular plate are compared. It is observed that the results from CUFSM closely coincide with the analytical solution. Also, it is noted that unlike the stability solutions the frequencies decrease monotonically to a plateau.

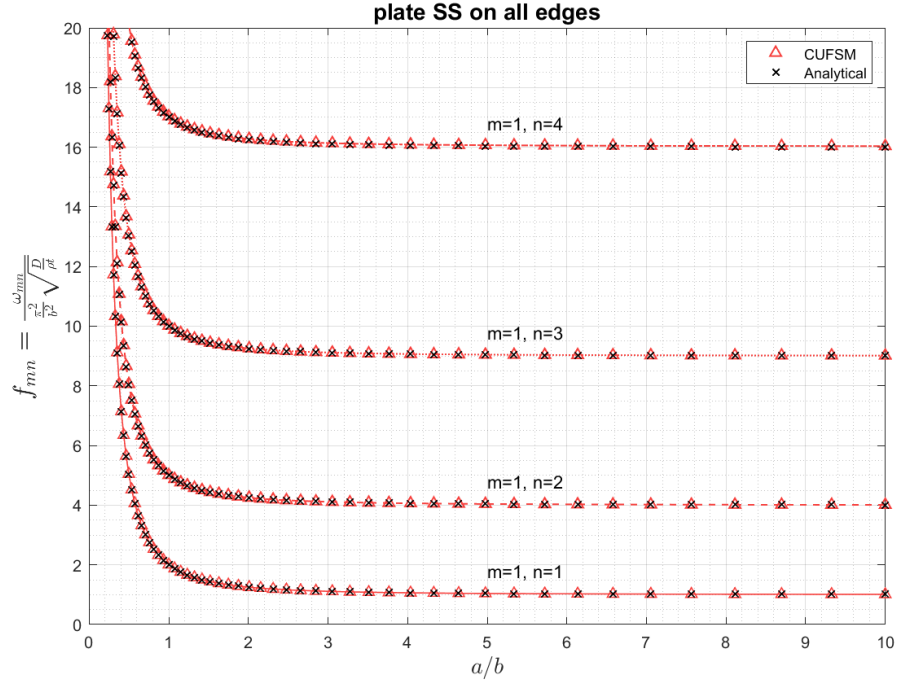


Figure 4: Plot comparing non-dimensional vibration frequencies k_{mn} between CUFSM and analytical solutions

4.2 Square plate fixed on all edges

A square plate with the same properties as the rectangular plate in the previous example, but with $a=b=100$ in. is modeled in CUFSM. The boundary condition is specified as ‘C-C’ and the nodes at the ends of the cross-section are defined with all degrees of freedom fixed (x, z, y, θ) to account for the plate being fixed on all the edges. Since the orthogonality properties cannot be applied to any boundary condition apart from the simply supported condition, multiple longitudinal terms are used here (in CUFSM this is defined by the vector $m_all = [1\ 2\ 3\ 4\ 5]$) to obtain accurate vibration frequencies. On performing the finite strip analysis, the results for the vibration mode shapes corresponding to $m=1$ and $n=1,2$ are shown in Fig. 5 and Fig. 6 and the vibration frequencies obtained are 3.485 Hz (21.9 rad/sec) and 7.09 Hz (44.6 rad/sec) respectively.

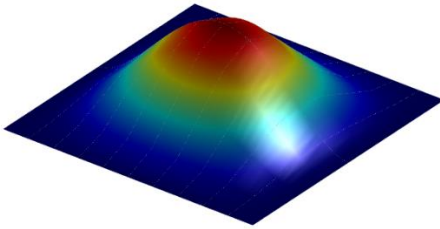


Figure 5: Mode shape (m,n)=1,1

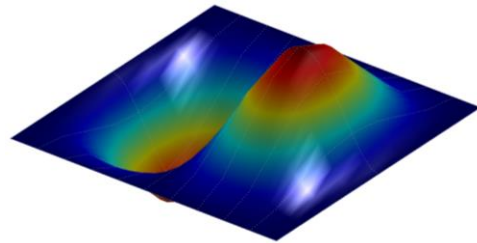


Figure 6: Mode shape for (m,n)=1,2

For a square plate fixed on all edges the analytical solution for the vibration frequency is not a closed-form expression. Hence, the vibration frequencies from CUFSM for a square plate ($a = b = 100$ in.) are compared with published solutions (see Cheung et al., 1998 and Wang et al., 2013) in Table 5 and the results are found to be in close agreement.

Table 5: Comparison between CUFSM and theoretical vibration frequencies for a fixed plate

(m, n)	Vibration Frequencies (rad/s)	
	CUFSM	Theoretical
(1,1)	21.9	21.6
(1,2)	44.6	44.1
(2,1)	45.1	44.3
(2,2)	66.4	65.1
(3,1)	79.9	80.1

4.3 Beam vibration frequencies

A simply supported and a cantilevered beam with a W24x68 cross-section are modeled in CUFSM and the vibration frequencies are obtained. The W24x68 model uses centerline dimensions and four strips in the flange and four strips in the web. The boundary conditions in CUFSM are specified 'S-S' and 'C-F' respectively.

The analytical solution for vibration frequency of a simply supported beam, corresponding to mode n (from Chopra et al., 2017) is:

$$\omega_n = \frac{n^2 \pi^2}{L^2} \sqrt{\left(\frac{EI}{\bar{m}}\right)} \quad (4.4)$$

Also, for a cantilevered beam the vibration frequencies corresponding to the first four modes are given as (from Chopra et al., 2017):

$$\omega_1 = \frac{3.516}{L^2} \sqrt{\frac{EI}{\bar{m}}} \quad \omega_2 = \frac{22.03}{L^2} \sqrt{\frac{EI}{\bar{m}}} \quad \omega_3 = \frac{61.70}{L^2} \sqrt{\frac{EI}{\bar{m}}} \quad \omega_4 = \frac{120.9}{L^2} \sqrt{\frac{EI}{\bar{m}}} \quad (4.5)$$

where L is the length of beam, E is the modulus of elasticity, I is the moment of inertia of the cross-section, \bar{m} is the mass per unit length = ρA where A is the area of the cross-section.

Fig. 7 and Fig. 8 compare the CUFSM and analytical vibration frequencies for a W24x68 simply supported beam and cantilevered beam respectively. CUFSM's vibration solution is in excellent agreement with the analytical solutions. For the simply supported case at short lengths in the higher modes CUFSM's frequency is slightly lower than the analytical solution indicating possible minor contributions from cross-section deformation. For the clamped case at short lengths CUFSM's higher mode solution is slightly above the analytical solution indicating that additional longitudinal terms are needed (greater than $m=5$) if more precise agreement is desired.

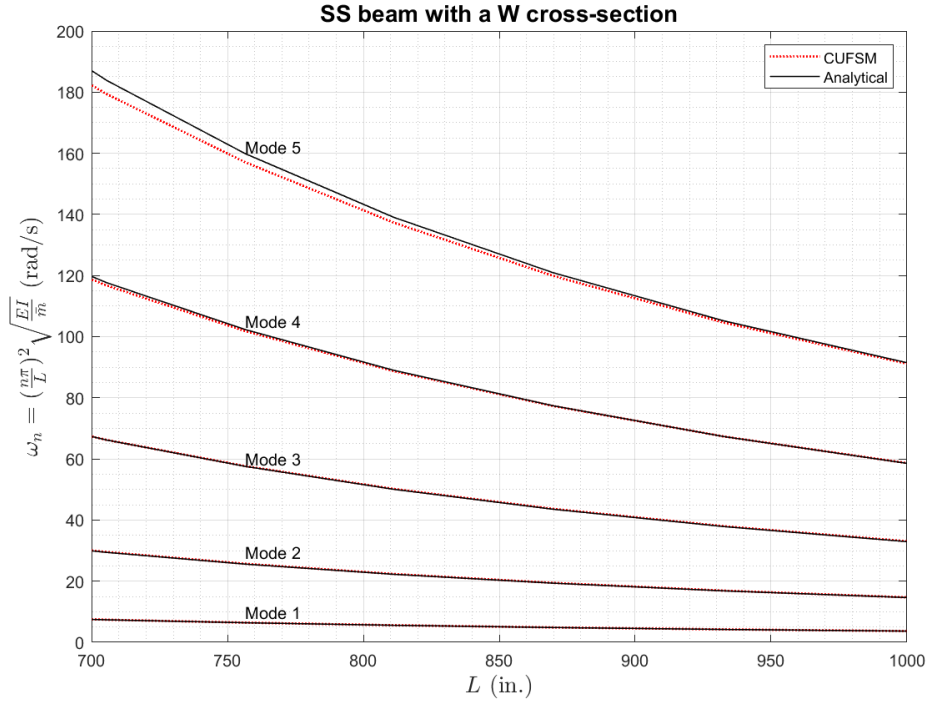


Figure 7: Comparison of CUFSM and analytical vibration frequencies for a W24x68 SS beam

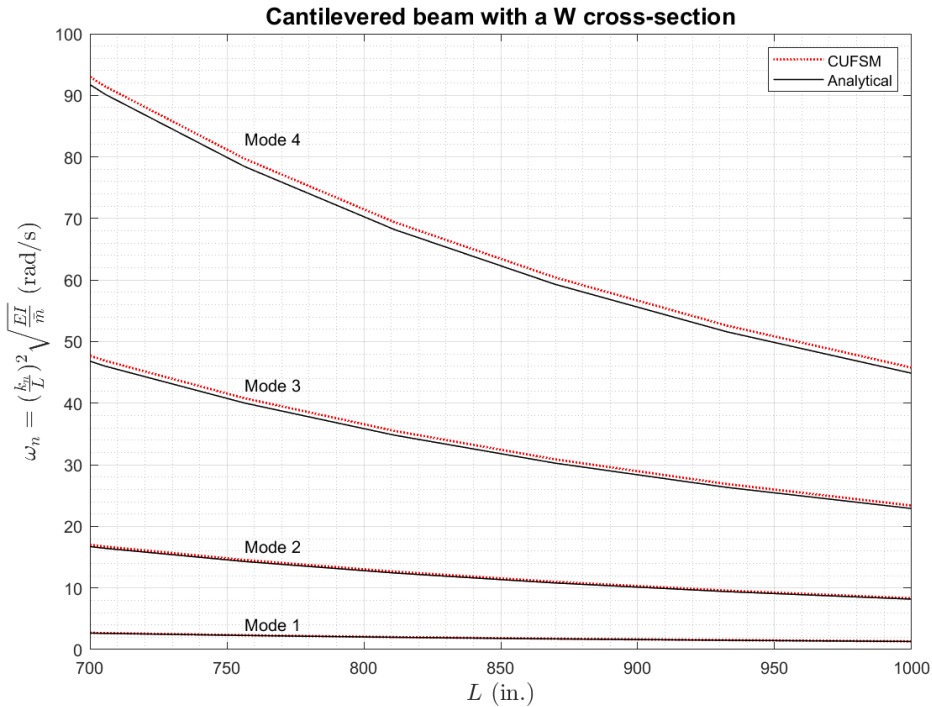


Figure 8: Comparison of CUFSM and analytical vibration frequencies for a W24x68 cantilevered beam

5. Example: Evaluation of prototype all-steel module

This section covers the evaluation of a prototype all-steel floor assembly for stability and vibration. This section provides details of the prototype floor assembly, potential loading methods for the

buckling analysis, critical buckling moments for local buckling and lateral torsional buckling, and the vibration frequencies for the beams, floor plate and the complete floor module.

5.1 Module

The prototype floor assembly consists of a pair of wide flange beams with a steel floor plate attached across the top. An assembly with a 3/8 in. thick floor plate on top of two W24x68s in the cross-section, as shown in Fig. 9 and Fig. 10 is modeled in CUFSM. The total length and width of the floor assembly are 480 in. (40 ft.) and 120 in. (10 ft.) respectively.

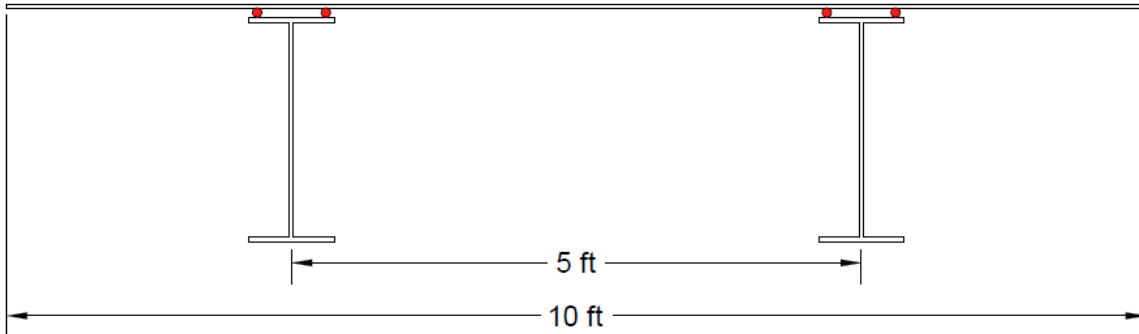


Figure 9: Cross-section of the prototype floor assembly

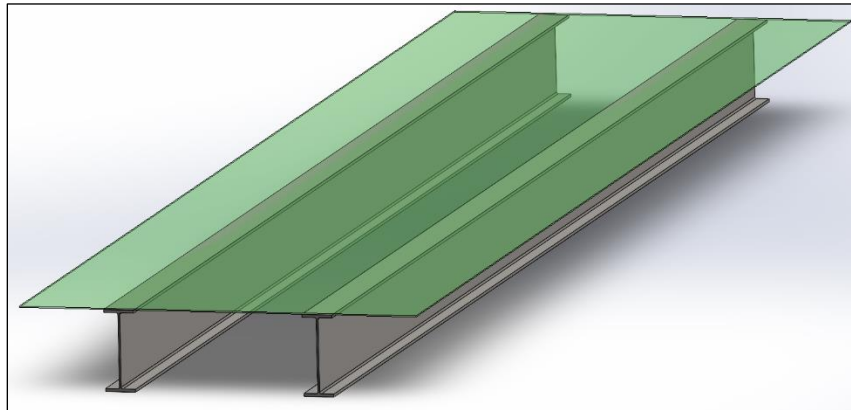


Figure 10: Isotropic view of the prototype floor assembly

5.2 Stability analysis

The finite strip method as implemented in CUFSM is utilized for the stability analysis. This method uses a plate element consistent with classical Kirchoff's plate theory and capable of capturing local buckling as well as all plate deformations associated with the assembly. However, CUFSM does not perform a first order analysis to determine internal stresses – the user provides the end tractions on the cross-section to be evaluated a priori. When using the semi-analytical finite strip method, only the first trigonometric term in the longitudinal direction is evaluated – creating what is known as the signature curve for a cross-section. For the evaluations conducted here a constant major axis bending reference moment of 1000 kip-in. is applied. Three methods of a priori internal stresses are considered (i) beams alone, as illustrated in Fig. 11 this provides an assessment of the beams without the top plate (ii) beams and stress free plate, as illustrated in Fig. 12 this provides and assessment where the top plate provides no composite action of load carrying

capability – but can provide lateral bracing to the top flange of the beams, and (iii) composite case, as illustrated in Fig. 13 where we assume a fully composite elastic stress distribution between the beam and the plate.



Figure 11: Two W-sections subject to major axis bending moment

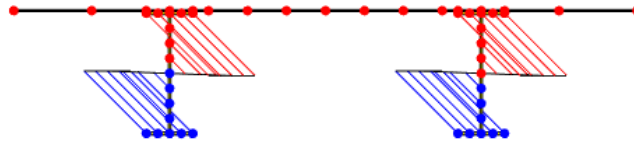


Figure 12: Stress free plate loading condition

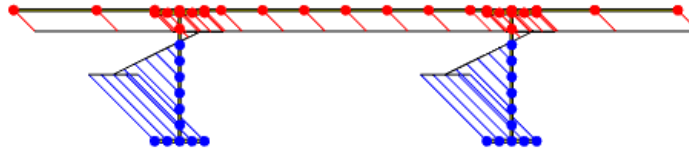


Figure 13: Composite loading condition

The signature curves from three different analysis methods are provided in Fig. 14. The plot provides the load factor (LF)-ratio of the critical moment (M_{cr}) to the applied moment ($M_{ref}=1000$ kip-in.) on the y-axis and the half wavelength in the x-axis. The first minima in the plot corresponds to the local buckling moments (M_{crl}) and the buckling moment at the length of the floor assembly (480 in.) corresponds to the lateral torsional buckling moments (M_{crlTB}). Further, the plot provides the buckled shapes against the undeformed shapes at half wavelengths corresponding to local and global buckling. The results from the stability analysis performed are summarized in the Table 6.

Table 6: Critical buckling moments from the stability analysis

	M_{crl}/M_{ref}	M_{crlTB}/M_{ref}
Two W24x68 beams	62	3.3
Stress Free Plate	94	1627
Composite Loading	6	87

Note* The applied moment, M_{ref} is 1000 kip-in.

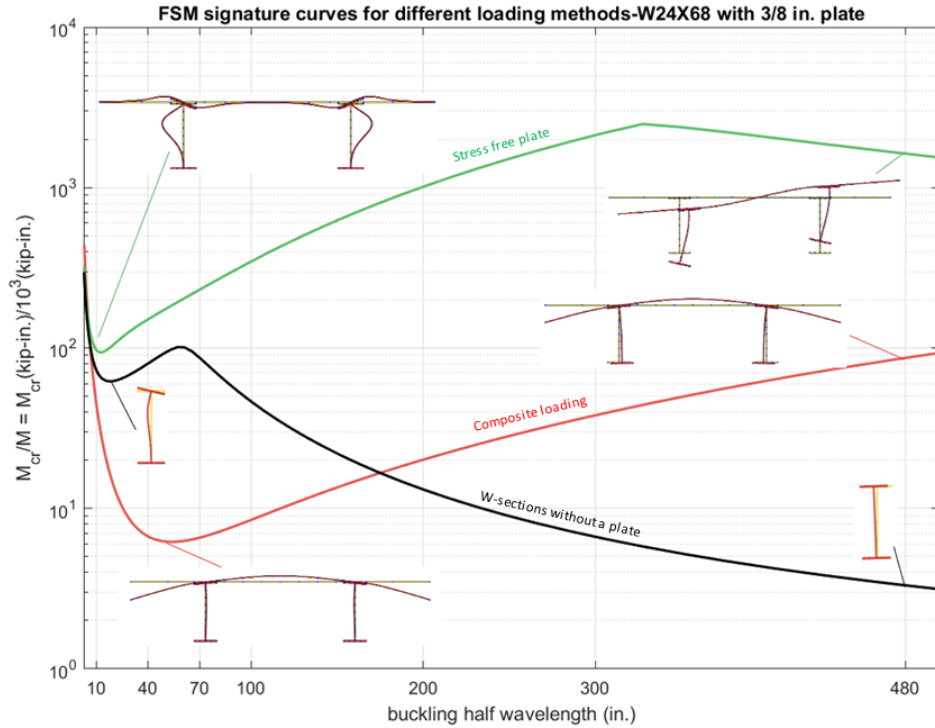


Figure 14: Signature curves from the stability analysis

From the signature curves of the stability analysis (Fig. 14) it is observed that the stress free plate condition displays the best performance in local and global buckling as it has the highest critical moment capacities. This is because the stress free plate provides lateral bracing of the top flanges of the W-sections and the lateral torsional buckling approximates to constrained axis flexural torsional buckling, with a small amount of torsional resistance. In the composite loading case, the critical local buckling moment is low – this would result in local buckling and unloading of the plate – nonlinear phenomena not captured in the eigenvalue stability analysis. The bare W24x68 beams, classified as compact sections for flexure (per AISC 360-16 table B4.1b), show good local buckling performance, but the critical buckling moments in lateral torsional buckling are relatively low indicating the need for bracing from the plate.

5.3 Vibration analysis

Vibration analysis is performed on the module and its constituent parts. Two different transverse edge boundary conditions are considered for the plates cantilevered edges: isolated and installed. The isolated condition simulates transportation and installation before being connected to other modules and is modeled as a free edge. The installed condition assumes a perfect connection to the neighboring module, enforced through symmetry boundary conditions on the free edge. In this initial vibration analysis the end boundary conditions are modeled as simply supported.

Having derived the finite strip method for vibration frequencies, CUFSM can be implemented to perform the vibration analysis for the prototype all-steel floor module. The first case considered is an L=480 in. long W24x68 beam without the floor plate, but laterally supported. The in-plane displacement is restrained for the W-section (x dof is fixed) to account for ideal lateral support

The mode shape for the fundamental mode is shown in Fig. 16a and the beam has a vibration frequency of 3.7 Hz for this case.

The second case considered is the 3/8 in. floor plate in the isolated and installed conditions. The plate shown in Fig. 15 is modeled in CUFSM with fixed degrees of freedom at the four weld points to account for the plate being connected to the W-section. The plate is examined under the isolated and installed conditions and the mode shapes are shown in Fig. 16d and Fig. 16e respectively. The vibration frequencies for the isolated and the installed plate are found to be 6.2 Hz and 8.2 Hz respectively.

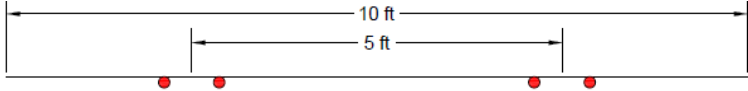


Figure 15: Floor plate with weld points

The final case is an evaluation of the vibration of the complete floor assembly under isolated and installed conditions. The vibration modes for the two conditions are shown in Fig. 16b and Fig. 16c with vibration frequencies of 4.7 Hz for the isolated and 6.7 Hz for the installed conditions.

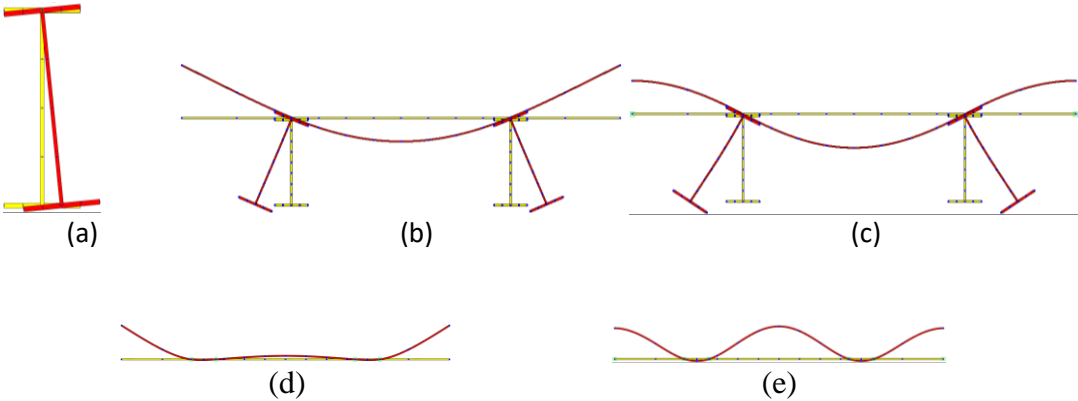


Figure 16: Mode shapes of (a) W24x68 beam (b) isolated floor module (c) installed floor module (d) isolated floor plate (e) installed floor plate

We can readily provide the isolated and installed vibration frequencies as a function of module length, as shown in Fig. 17. The results indicate the dominance of the beam vibration modes, and only at short supported lengths does the frequency increase substantially.

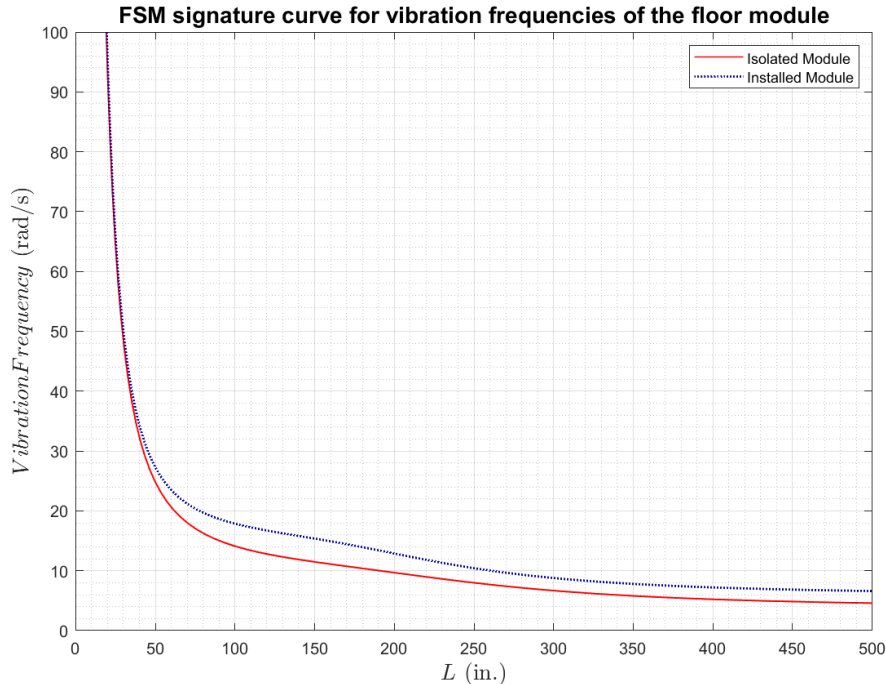


Figure 17: Signature curves from the vibration analysis

From the vibration analysis (Fig. 17) it can be noticed that the installed modules have a higher vibration frequency than the isolated modules, but values are still relatively low at expected module lengths. Actual modules will have end boundary conditions with partial restraint, additional elements such as raised access floors that may potentially increase the damping, and other features that may lead to improved performance. Additional evaluation is required for a more comprehensive vibration serviceability assessment.

6. Discussion

Eigen buckling and vibration solutions are not themselves a complete stability or vibration assessment. Elastic buckling is only the first step towards successful stability assessment, but having complete local and global elastic buckling solutions that are easy to implement and true to the details of the cross-section being studied has proven useful in structural design. Extending CUFSM to the eigenvalue vibration problem has the same intent – full assessment requires understanding accelerations and, in many cases, significant judgment is also required as encapsulated in supporting documents such as AISC’s Design Guide 11 (Murray et al., 2016). Nonetheless, accurate vibration frequencies that can account for complicated sections and inter-connections efficiently, have a role to play in speeding and improving vibration assessment.

Finite strip models use substantially fewer DOF per model than equivalent shell finite element models. For the 480 in. long all-steel floor modules the finite strip model uses 176 DOF (a total of 12 strips for the plate, 16 strips for each beam, 4 DOF per strip, and only one longitudinal DOF). For the shell finite element (FE) model, assuming a 2:1 longitudinal aspect ratio is acceptable, and use of linear shell elements as opposed to the higher order cubic strips is acceptable, then an equivalent shell FE model would use at least 14,080 DOF, or 80× more. While today both can run on a laptop, the finite strip solution is nearly instantaneous, and requires little input data – and the underlying mechanics are the same. In fact, the validation studies show that the elastic finite strip

matrices combined with consistent mass matrices can essentially reproduce both local plate and global member vibration solutions. This same fact for stability solutions has allowed finite strip to provide an important middle ground between analytical solutions and complex shell FE models.

The prototype all-steel modular floor assembly is a potential new innovation to increase the speed of structural steel building construction. While simple in form, the module attempts to balance a number of competing factors between design, fabrication, erection, and final installed performance. Final form of the module, and final sizes of the constituent parts are not yet established. The tools developed here, combined with experimental testing, and detailed shell finite element models all have a role to play in developing such new innovations.

Within the context of this paper the team is working to bring the new vibration solution into the CUFSM interface and publicly release this functionality. In addition, we are looking at (a) deeper examinations of the bracing performance of the flat plate against the selected beams and how to bring this form of bracing into steel design, and (b) the vibration performance of the assembly and how to meaningfully account for end continuity and other elements in the eigenvalue vibration assessment.

7. Conclusions

The finite strip method can be an efficient alternative to shell finite element models. CUFSM provides stability analysis of cross-sections using the finite strip method and has proven useful in assessment and design. CUFSM's finite strip solution was extended to include free vibration and the solution of the eigen frequencies and vibration mode shapes. The solution employs consistent mass matrices and the same stiffness matrices as used in stability assessment. The only new input required is the density of the materials utilized. The implemented solution is successfully validated against both classical plate and beam solutions. The developed tool allows for rapid assessment of eigen stability and vibration – such assessment of a newly proposed prototype all-steel floor module is performed. The prototype module consists of two W-section beams and an attached top plate – both the stability and vibration performance are sensitive to the geometry of the selected members and the inter-connect between the plate and beams. The developed tool provides a platform for rapid future assessment of the module. Work to bringing the new capabilities of CUFSM into the publicly available open-source interface, and further assessment of the prototype floor module are all underway.

Acknowledgements

This material is based upon work supported by the Charles F. Pankow Foundation, the American Institute of Steel Construction (AISC), MKA Foundation, NUCOR Corporation, Schuff Steel, and Johns Hopkins University. This work is being conducted in coordination with the AISC “Need for Speed” initiative under the auspices of the Steel Diaphragm Innovation Initiative (SDII). The authors thank all of the SDII collaborators for their contributions and ideas, including Ron Klemencic, Joshua Mouras, and Juzer Millwala of MKA. Any findings, conclusions or recommendations expressed in this paper are those of the authors and do not necessarily reflect the views of any sponsors.

References

- Bradford, M.A., and Azhari, M., *Buckling of plates with different end conditions using the finite strip method*. Computers & Structures, 1995. 56(1): p. 75-83.
- Cheung, Y. K., Tham, L. G., *Finite Strip Method*. CRC Press, 1998.
- Cheung, M. S., and Cheung, Y.K. 1971. "Natural Vibrations of Thin, Flat-Walled Structures with Different Boundary Conditions." *Journal of Sound and Vibration* 18 (3): 325–37. [https://doi.org/10.1016/0022-460X\(71\)90705-X](https://doi.org/10.1016/0022-460X(71)90705-X).
- Chopra, A., *Dynamics of structures*, 5th ed. 2017.
- Hancock, G., *Design of cold-formed steel structures*, 5th ed. Australian Steel Institute. [Online]. Available: <https://www.steel.org.au/resources/book-shop/design-of-cold-formed-steel-structures-5th-edition-bundle-hardcopy-and-ebook/>
- Li, Z., Schafer, B.W. (2010). "Buckling analysis of cold-formed steel members with general boundary conditions using CUFSM: conventional and constrained finite strip methods." *Proceedings of the Twentieth International Specialty Conference on Cold-Formed Steel Structures*, Saint Louis, MO.
- Li, Z., and Schafer, B.W., *Application of the finite strip method in cold-formed steel member design*. Journal of Constructional Steel Research, 2010. 66(8-9): p. 971-980.
- Li, Z., and Schafer, B.W., *Finite Strip Stability Solutions for General Boundary Conditions and the Extension of the Constrained Finite Strip Method*. in Trends in Civil and Structural Engineering Computing. 2009. Stirlingshire, UK: Saxe-Coburg Publications.
- Li, Z., and Schafer, B.W., *The constrained finite strip method for general end boundary conditions*, in Structural Stability Research Council - Proceedings of the 2010 Annual Stability Conference. 2010: Orlando, FL, USA. p. 573-591.
- Li, Z., 2011. Finite Strip Modeling of Thin-Walled Members (PhD Dissertation). Johns Hopkins University, Baltimore, MD.
- Murray, T.M., Allen, D.E., Ungar, E.E. and Davis, D.B., 2016. *Vibrations of steel-framed structural systems due to human activity: Second Edition*. American Institute of Steel Construction, 2016.
- Schafer, B.W. and Ádány, S., *Buckling analysis of cold-formed steel members using CUFSM: Conventional and constrained finite strip methods.*, in *18th International Specialty Conference on Cold-Formed Steel Structures: Recent Research and Developments in Cold-Formed Steel Design and Construction*. 2006. p. 39-54.
- Szilard, Rudolph. 2004. *Theories and Applications of Plate Analysis*. Hoboken, NJ, USA: John Wiley & Sons, Inc. <https://doi.org/10.1002/9780470172872>.
- Timoshenko, S.P., Gere, J.M., Prager, W., 1962. Theory of Elastic Stability, Second Edition. Journal of Applied Mechanics 29, 220–221. <https://doi.org/10.1115/1.3636481>
- Wang, C. Y., *Structural Vibration: Exact Solutions for Strings, Membranes, Beams, and Plates*, 1st ed. CRC Press, 2013.
- "ANSI/AISC 360-16 Specification for Structural Steel Buildings." American Institute of Steel Construction, Inc., 2016.
- "CUFSM – CROSS-SECTION ELASTIC BUCKLING ANALYSIS Constrained and Unconstrained Finite Strip Method." [Online]. Available: <https://www.ce.jhu.edu/cufsm/>
- "Design Guide 11: Floor Vibrations Due to Human Activity." American Institute of Steel Construction, Inc., 2003.
- "Lumped and Consistent Mass Matrices." <https://quickfem.com/wp-content/uploads/IFEM.Ch31.pdf>